

Analysis of Material Effect on Rail Impedance

Mehran Mirzaei

faculty of electrical engineering, department of measurement
czech technical university
Prague, Czech Republic
mirzameh@fel.cvut.cz

Pavel Ripka

faculty of electrical engineering, department of measurement
czech technical university
Prague, Czech Republic
ripka@fel.cvut.cz

Abstract—In this paper, two different solid iron materials are used for two different size rails. The internal impedances, resistances and inductances of the rails are evaluated and analyzed with time harmonic and time stepping finite element methods. Two solid iron materials have different B - H curves and electrical conductivities. The analysis will be presented for different currents at different frequencies, 10 Hz - 10 kHz. The inductance analysis using finite element method is also performed under simultaneous large DC signal and small AC signal.

Keywords—rail, material, impedance, analysis

I. INTRODUCTION

The rails are electrically used for traction power currents and signaling circuits. Therefore impedance analyses of the rails are critical for power system analysis and accurate control signaling. The rail inductance value is required for signaling circuit analysis. Rail impedance and earth impedance is used in the power system dynamic analysis during unbalanced conditions.

AC and DC analysis of rail impedance are both required for AC and DC systems. Using power electronics switching in DC traction systems causes both DC signals and AC signals simultaneously in the rail, which means that incremental permeability is required for impedance analysis for AC component. Same phenomena are happening for impedance analysis of the rail for signaling circuits when power currents exist in the rails.

Several papers were presented for impedance analysis of iron rails [1]-[11]. Few papers presented detailed analysis of the rails impedances [8] - [10], which lack rail material effect on the rails impedances. References [8] - [10] study nonlinearity and hysteresis effects on the rail impedances but they do not precisely illustrate different materials effects on the rails impedances.

Impedance of iron rails are highly dependent on the current and the frequency, which is caused by nonlinear B - H curve and high electrical conductivity of the solid iron rail. Two materials with different B - H curves and electrical conductivities are used for simulations in this paper. Two iron rails are used with different dimensions.

Two simplified circular and rectangular shapes equivalent models will be presented for each rail, which will be analyzed with finite element method (FEM) and analytical method for using as equivalent models of the complicated shapes of the rails.

II. DIMENSIONS AND MATERIALS

A. Dimensions and Material data

The rails dimensions are shown in Fig. 1 for two rail models, A and B.

Two different solid iron materials 1 and 2 are used, with corresponding μ_r - H curves (relative magnetic permeability versus magnetic field strength) shown in Fig. 2. Electrical conductivities for materials 1 and 2 are 4.45 MS/m and 5.07 MS/m, respectively.

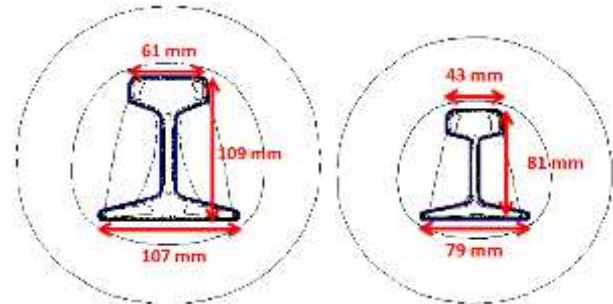


Fig. 1. Rails dimensions and corresponding magnetic flux distribution at 50 Hz - Model A (left) and Model B (right)

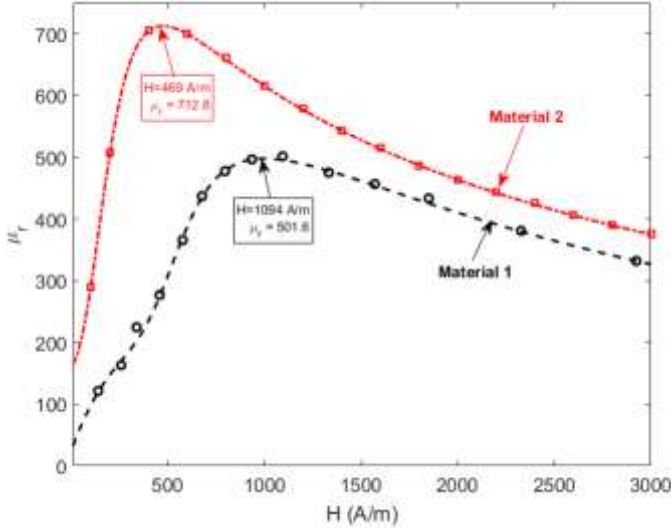


Fig. 2. Materials 1 and 2 - μ_r - H

III. APPROXIMATE EQUIVALENT MODELS

Two equivalent models are considered for the rails configuration in Fig. 1. First equivalent model is circular shape and second equivalent model is square shape, for which edge and corner effects could be seen unlike circular shape model. The dimensions of equivalent models are calculated from circumferences and areas of the rails. Rail area value is used for equivalent models dimensions calculations when skin effect is low and current is smoothly distributed in the rail cross section. Rail circumference value is applied for high skin effect to calculate equivalent models dimensions. Equivalent radius, r_e and edge, a_e sizes for circular shape and square shape models are as following in (1) and (2):

$$r_{e,S} = \left(\frac{S}{\pi} \right)^{0.5} \quad (1)$$

$$r_{e,C} = \frac{C}{2\pi}$$

$$a_{e,S} = S^{0.5} \quad (2)$$

$$a_{e,C} = \frac{C}{4}$$

where, S and C are area and circumference of the rails cross section.

Cross section area and circumference of rails A and B are 3837.3 mm², 473.77 mm, 2070.8 mm² and 356.41 mm.

A. Circular shape models

Equivalent radii, $r_{e,S}$, $r_{e,C}$ for rails A and B are calculated using (1) equal to 34.95 mm, 75.4 mm, 25.67 mm and 56.72 mm, respectively. Fig. 3 shows equivalent circular models with half model configuration for rails A and B.

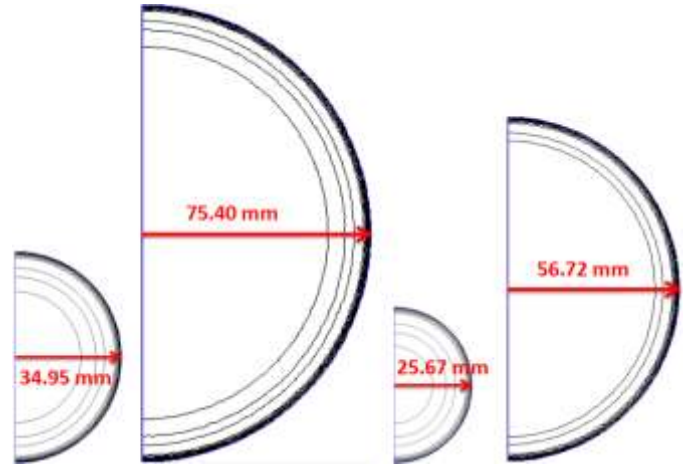


Fig. 3. Equivalent circular models radius and magnetic flux distribution at 50 Hz- from left to right, equivalent area to rail A, equivalent circumference to rail A, equivalent area to rail B and equivalent circumference to rail B

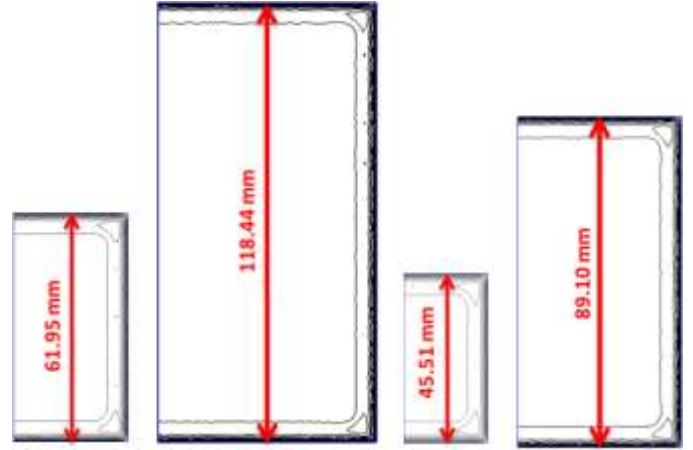


Fig. 4. Equivalent square models edge and magnetic flux distribution at 50 Hz- from left to right, equivalent area to rail A, equivalent circumference to rail A, equivalent area to rail B and equivalent circumference to rail B

B. Square shape models

Equivalent edges, $a_{e,S}$, $a_{e,C}$ for rails A and B are calculated using (1) equal to 61.95 mm, 118.44 mm, 45.51 mm and 89.10 mm, respectively. Fig. 4 shows equivalent square models with half model configuration for rails A and B.

Table I shows finite element analysis of the resistances and the inductances of the rails with relative magnetic permeability, $\mu_r = 250$ and two different conductivities. The conductivities have 12% difference, which has significant influence about 3.5% - 9% on resistances and inductances at 10 Hz and 50 Hz.

TABLE I. RESISTANCE AND INDUCTANCE PER METER RESULTS FOR REAL MODELS USING FEM

$\mu_r = 250$	Rail A		Rail B	
	4.45 MS/m	5.07 MS/m	4.45 MS/m	5.07 MS/m
R,DC	58.6 $\mu\Omega$	51.4 $\mu\Omega$	108.5 $\mu\Omega$	95.3 $\mu\Omega$
L,DC	2.61 μH	2.61 μH	2.73 μH	2.73 μH

$\mu_r = 250$	Rail A		Rail B	
	4.45 MS/m	5.07 MS/m	4.45 MS/m	5.07 MS/m
R, 10Hz	101.7 $\mu\Omega$	94.2 $\mu\Omega$	154.0 $\mu\Omega$	140.1 $\mu\Omega$
L, 10Hz	1.41 μH	1.36 μH	1.63 μH	1.57 μH
R, 50Hz	226.1 $\mu\Omega$	211.8 $\mu\Omega$	296.3 $\mu\Omega$	278.8 $\mu\Omega$
L, 50Hz	0.71 μH	0.66 μH	0.93 μH	0.88 μH

TABLE II. RESISTANCE AND INDUCTANCE PER METER RESULTS FOR EQUIVALENT CIRCULAR MODELS USING FEM

$\sigma_i = 4.45$ MS/m $\mu_r = 250$	Rail A		Rail B	
	Equi. Area	Equi. circu.	Equi. area	Equi. circu.
R, DC	58.6 $\mu\Omega$	12.6 $\mu\Omega$	108.6 $\mu\Omega$	22.2 $\mu\Omega$
L, DC	12.5 μH	12.5 μH	12.5 μH	12.5 μH
R, 10Hz	230.0 $\mu\Omega$	102.9 $\mu\Omega$	321.4 $\mu\Omega$	137.9 $\mu\Omega$
L, 10Hz	3.40 μH	1.58 μH	4.61 μH	2.10 μH
R, 50Hz	496.5 $\mu\Omega$	228.7 $\mu\Omega$	684.8 $\mu\Omega$	301.5 $\mu\Omega$
L, 50Hz	1.52 μH	0.70 μH	2.06 μH	0.94 μH

TABLE III. RESISTANCE AND INDUCTANCE PER METER RESULTS FOR EQUIVALENT SQUARE MODELS USING FEM

$\sigma_i = 4.45$ MS/m $\mu_r = 250$	Rail A		Rail B	
	Equi. area	Equi. circu.	Equi. area	Equi. circu.
R, DC	58.6 $\mu\Omega$	16.0 $\mu\Omega$	108.5 $\mu\Omega$	28.3 $\mu\Omega$
L, DC	11.04 μH	11.04 μH	11.04 μH	11.04 μH
R, 10Hz	209.7 $\mu\Omega$	104.7 $\mu\Omega$	295.6 $\mu\Omega$	141.5 $\mu\Omega$
L, 10Hz	3.01 μH	1.58 μH	4.07 μH	2.10 μH
R, 50Hz	444.6 $\mu\Omega$	227.7 $\mu\Omega$	614.7 $\mu\Omega$	305.0 $\mu\Omega$
L, 50Hz	1.35 μH	0.71 μH	1.84 μH	0.94 μH

The FEM results for equivalent circular and square models are presented in Tables II and III. The approximate models equivalent to cross section areas of the rails are not suitable for resistance and inductance analysis for AC currents, because the currents and fields are mostly located near the skin of the models. Therefore, the models equivalent to circumferences of the rail are more practical.

The approximate models equivalent to rails circumference show promising results in Table II and III for higher frequencies in comparison with real rail impedance analysis in Table I. Fig. 5 shows magnetic flux distributions in the rail models and equivalent models at DC and 50 Hz currents. Magnetic flux distributions at 50 Hz are located close to the rail wall and magnetic fields intensities are independent of rail shape unlike DC field model. Therefore the approximate models results are coinciding well with real rail results at AC currents.

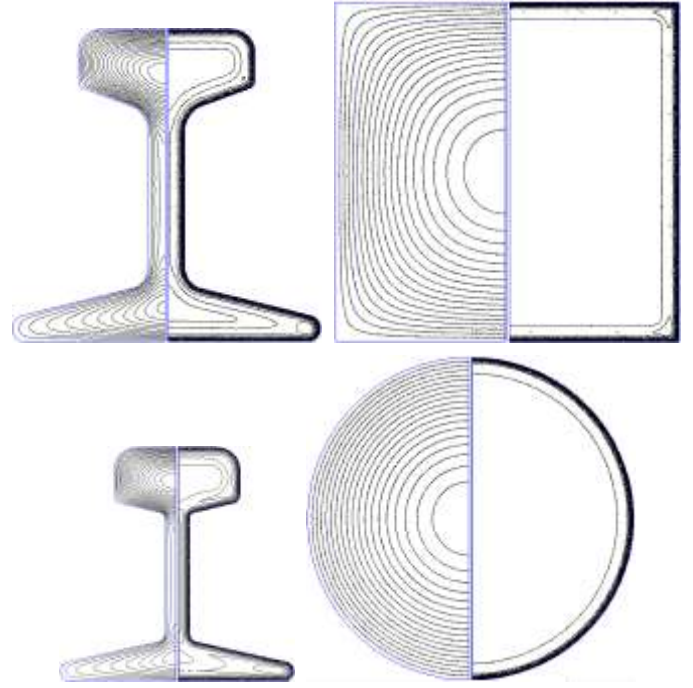


Fig. 5. Magnetic flux distribution at DC (left) and 50 Hz (right) in real model of rail A and equivalent models of rail A (up with square equivalent) and rail B (bottom with circular equivalent) for equal circumference

C. Analytical Formulations

The electric field, E_z in the circular conductor and resulting internal impedance, Z_{in} for the circular conductor with outer radius r is given as following [12]:

$$Z_{in} = \frac{E_z(r)}{I} = \frac{\alpha}{\sigma_i \cdot 2 \cdot \pi \cdot r} \cdot \frac{\text{Besseli}(0, \alpha \cdot r)}{\text{Besseli}(1, \alpha \cdot r)}$$

$$\alpha = \sqrt{j\omega\sigma_i\mu} = \frac{1+j}{\delta}, \quad (\delta = \sqrt{\frac{2}{\omega\sigma_i\mu}})$$

$$\mu = \mu_r \cdot \mu_0, \quad \omega = 2 \cdot \pi \cdot f$$

where, I , σ_i , μ_0 , μ_r and f are applied current, solid iron electrical conductivity, free space permeability, relative magnetic permeability and frequency, respectively. δ is the classical skin depth formula.

The simpler formula for equivalent circular model impedance could be as following [12]:

$$Z_{in} = R + j\omega L, \quad R_{dc} = \frac{1}{\sigma_i \cdot \pi r^2}$$

$$R = R_{dc} \cdot \left(\frac{r}{2\delta} + \frac{1}{4} + \frac{3\delta}{32r} \right)$$

$$L = \frac{R_{dc}}{\omega} \cdot \left(\frac{r}{2\delta} - \frac{3\delta}{32r} \right)$$

It is assumed that magnetic field is tangential to outer surface of solid iron equivalent square model because of high

magnetic permeability of solid iron relative to the surrounding air region [12]. The approximate formula for internal impedance, Z_{in} is given in (5) with square edge value, a , which is the average integral of electric field on the outer surface of the rectangular conductor:

$$Z_{in} = \frac{\oint E_z \cdot dl}{4 \cdot a} = \frac{1}{\sigma_i} \cdot (2 + a \cdot \coth\left(\alpha \cdot \frac{a}{2}\right) \cdot \alpha) / (4 \cdot a^2) \quad (5)$$

The simpler formula for the equivalent square model impedance could be as following:

$$\begin{aligned} Z_{in} &= R + j\omega L, \quad R_{dc} = \frac{1}{\sigma_i \cdot a^2} \\ R &= R_{dc} \cdot \left(\frac{1}{2} + \frac{a}{4\delta}\right) \\ L &= \frac{R_{dc}}{\omega} \cdot \frac{a}{4\delta} \end{aligned} \quad (6)$$

The analytical results for resistances and inductances of approximate circular and square models are presented in Tables IV and V. They coincide well with FEM results, which show high precision of analytical models. The simpler formulas in (4) and (6) are also precise despite their simple function form.

TABLE IV. RESISTANCE AND INDUCTANCE PER METER RESULTS FOR EQUIVALENT CIRCULAR MODELS USING ANALYTICAL

$\sigma_i = 4.45$ MS/m $\mu_r = 250$	Rail A		Rail B	
	Using (3)	Using (4)	Using (3)	Using (4)
R, 10Hz	102.6 $\mu\Omega$	102.6 $\mu\Omega$	137.9 $\mu\Omega$	137.9 $\mu\Omega$
L, 10Hz	1.58 μH	1.58 μH	2.10 μH	2.10 μH
R, 50Hz	225.5 $\mu\Omega$	225.5 $\mu\Omega$	301.1 $\mu\Omega$	301.1 $\mu\Omega$
L, 50Hz	0.71 μH	0.71 μH	0.94 μH	0.94 μH

TABLE V. RESISTANCE AND INDUCTANCE PER METER RESULTS FOR EQUIVALENT SQUARE MODELS USING ANALYTICAL

$\sigma_i = 4.45$ MS/m $\mu_r = 250$	Rail A		Rail B	
	Using (5)	Using (6)	Using (5)	Using (6)
R, 10Hz	107.5 $\mu\Omega$	107.5 $\mu\Omega$	146.3 $\mu\Omega$	146.3 $\mu\Omega$
L, 10Hz	1.58 μH	1.58 μH	2.10 μH	2.10 μH
R, 50Hz	230.4 $\mu\Omega$	230.4 $\mu\Omega$	309.6 $\mu\Omega$	309.6 $\mu\Omega$
L, 50Hz	0.71 μH	0.71 μH	0.94 μH	0.94 μH

IV. NONLINEAR ANALYSIS

A. DC Current

Fig. 6 shows inductances at DC currents. The inductances profile versus current is similar to μ_r - H curves in Fig. 2 because the internal inductance is proportional to relative magnetic permeability. The corresponding curve fitting function is as following for inductance versus current:

$$L_{DC} = \frac{p_1 \cdot x^2 + p_2 \cdot x + p_3}{x^2 + q_1 \cdot x + q_2} (\mu\text{H}), \quad x = \frac{I_{DC} - 476.7}{436.3} \quad (7)$$

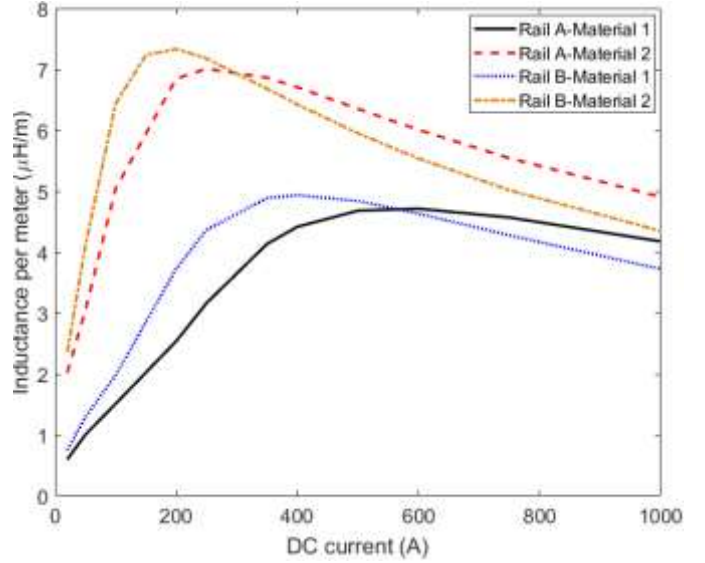


Fig. 6. DC inductance of the rails versus DC current (curve fitting function parameters: Rail A Material 1 ($p_1=1.825, p_2=7.608, p_3=6.733, q_1=1.324, q_2=1.447$), Rail A Material 2 ($p_1=2.393, p_2=11.62, p_3=10.17, q_1=2.24, q_2=1.575$), Rail B Material 1 ($p_1=1.492, p_2=7.264, p_3=6.474, q_1=1.657, q_2=1.315$), Rail B Material 2 ($p_1=1.734, p_2=11.26, p_3=10.34, q_1=2.489, q_2=1.708$))

B. AC Current

The time stepping FEM is required to calculate accurately nonlinear eddy current analysis. For example, the resistance can be calculated from time stepping analysis as following:

$$R = \frac{P_L}{0.5 \cdot I^2} \quad (8)$$

where, P_L is the average of power losses of the rail at AC current. Time stepping FEM is time consuming, which could be replaced by nonlinear time harmonic FEM with some approximations.

Magnetic flux density, B and magnetic field strength, H cannot be sinusoidal in the same time because B - H curve is nonlinear. It is assumed that H is sinusoidal and B is not sinusoidal. In order to compute magnetic fields in time harmonic domain, only fundamental component of B is considered and other harmonics are ignored due to the negligible effect on the eddy current losses [13].

Fig. 7 shows losses for rail A with material 1 at 50 Hz and current amplitude 500 A. The average value for losses is 32.66 W, which means resistance of the rail equal to 261 $\mu\Omega$ /m. The calculated resistance from time harmonic FEM is almost the same value as 261 $\mu\Omega$ /m from time stepping FEM. Fig. 8-Fig. 11 show resistances and inductances of rails A and B with two materials 1 and 2. The resistances increase and inductances decrease with increasing frequency due to the skin effect. The resistances and inductances values and their maxima are highly dependent on the materials. The corresponding currents for maximum values of resistances and

inductances are independent of frequencies and they are almost the same for the rails A and B. The rail B is smaller and its resistance and inductance are larger than resistance and inductance of rail A. The effects of materials decrease at higher currents because of saturation effects on the relative permeability. The permeabilities differences are decreasing with increasing currents and corresponding magnetic fields.

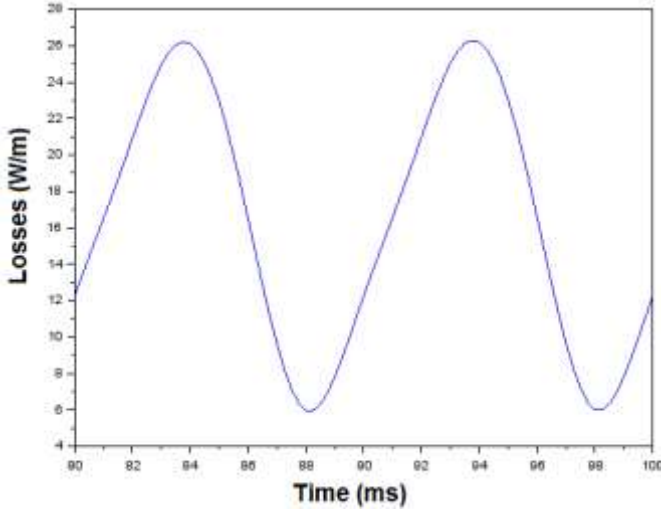


Fig. 7. Losses versus time for rail A with material 1 at 50 Hz and current amplitude 500 A - time stepping finite element method

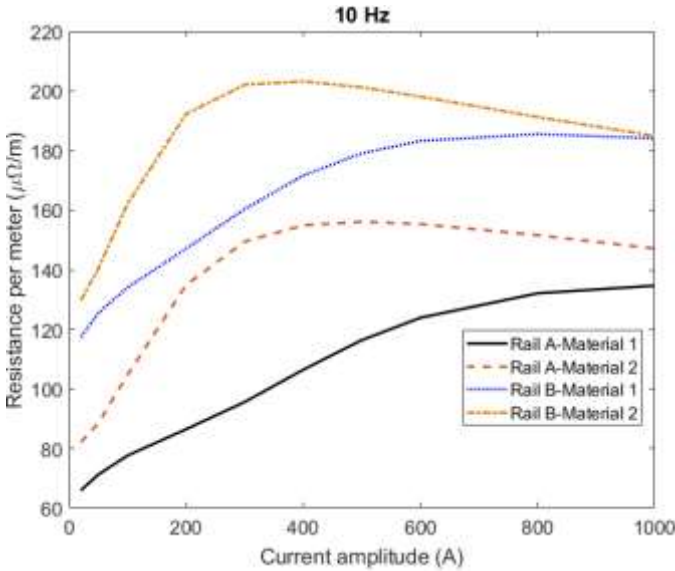


Fig. 8. AC resistance of the rails at 10 Hz

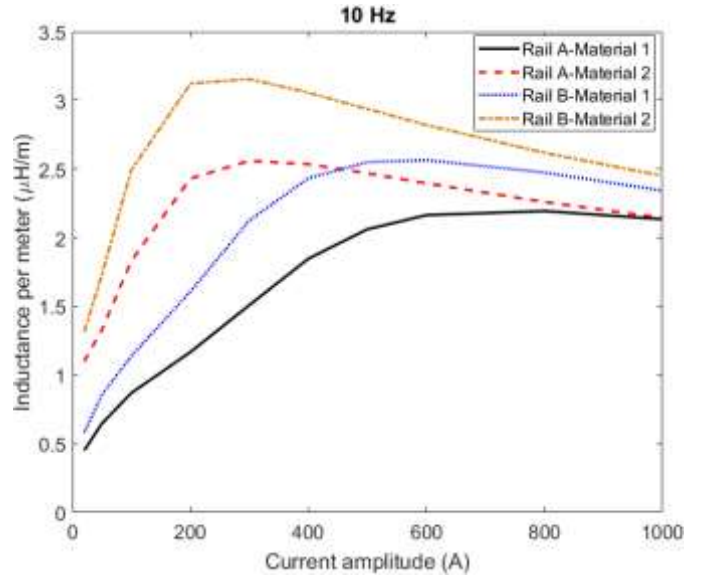


Fig. 9. AC inductance of the rails at 10 Hz

In order to consider hysteresis effects, hysteresis angle is taken into account in time harmonic FEM as following [13]-[14]:

$$\varphi_h(B) = \frac{\mu_e(B)}{\mu_{e-\max}} \cdot \varphi_{h-\max} \quad (9)$$

where, $\varphi_h(B)$, $\mu_e(B)$, $\mu_{e-\max}(B)$ and $\varphi_{h-\max}$ are flux density dependent hysteresis angle, flux density dependent efficient relative permeability, maximum efficient relative permeability and maximum hysteresis angle.

The calculated resistances and inductances at 500 A are shown in Table VI when maximum hysteresis angle, $\varphi_{h-\max} = 30$ Deg. is considered.

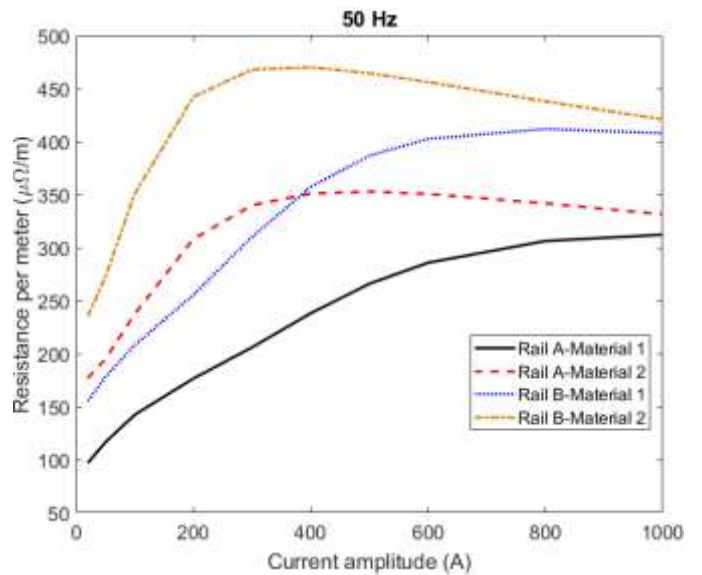


Fig. 10. AC resistance of the rails at 50 Hz

$$H_o = \frac{I}{C} \quad (10)$$

Table VII presents resistances and inductances at 10 kHz with different differential permeabilities. The resistances are much higher and inductances are much lower in comparison with low frequencies, 10 Hz and 50 Hz.

TABLE VII. RESISTANCE AND INDUCTANCE PER METER RESULTS USING ANALYTICAL METHOD AT 10 KHZ

500 A	Rail A		Rail B	
	Material 1	Material 2	Material 1	Material 2
R, $\mu_a=250$	3151.5 $\mu\Omega$	2952.0 $\mu\Omega$	4192.8 $\mu\Omega$	3927.2 $\mu\Omega$
L, $\mu_a=250$	0.050 μH	0.047 μH	0.067 μH	0.062 μH
R, $\mu_a=750$	5452.7 $\mu\Omega$	5107.9 $\mu\Omega$	7251.7 $\mu\Omega$	6793.0 $\mu\Omega$
L, $\mu_a=750$	0.087 μH	0.081 μH	0.115 μH	0.108 μH

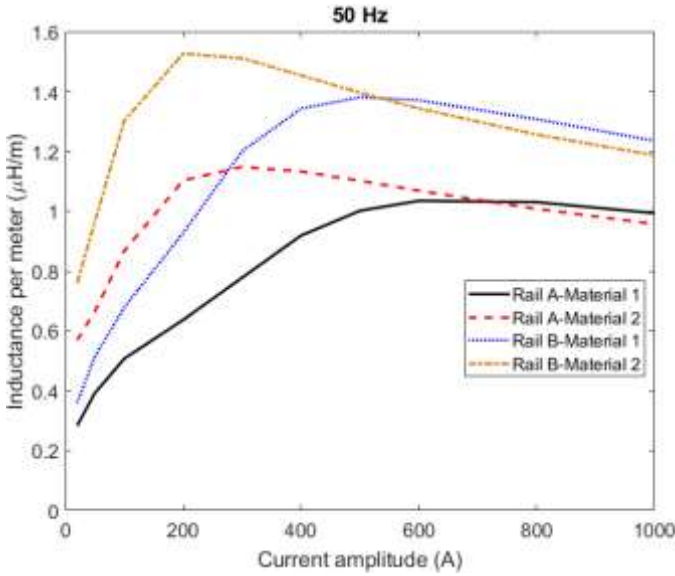


Fig. 11. AC inductance of the rails at 50 Hz

TABLE VI. RESISTANCE AND INDUCTANCE PER METER RESULTS USING FEM WITH HYSTERESIS EFFECTS

500 A	Rail A		Rail B	
	Material 1	Material 2	Material 1	Material 2
R, 10Hz	148.6 $\mu\Omega$	189.0 $\mu\Omega$	223.5 $\mu\Omega$	247.3 $\mu\Omega$
L, 10Hz	1.60 μH	1.77 μH	1.91 μH	2.17 μH
R, 50Hz	323.8 $\mu\Omega$	422.6 $\mu\Omega$	473.2 $\mu\Omega$	548.9 $\mu\Omega$
L, 50Hz	0.77 μH	0.80 μH	1.01 μH	1.03 μH

V. SMALL SIGNAL ANALYSIS

Impedance analysis of the rail for signaling circuits when DC power currents exist in the rails are evaluated. Signaling currents in comparison with power currents for railways is negligible, which small signal analysis could be used for impedance analysis of rails at high frequencies [8]. Differential or incremental magnetic permeability, $\mu_d \left(\frac{1}{\mu_0} \cdot \frac{dB}{dH} \right)$ is calculated for resistance and inductance analysis in the simulations (Fig. 12). It could be assumed that magnetic fields are mostly concentrated on the very small region on the skin of the rail due to the very high frequency of signaling circuits. Therefore magnetic permeability is considered constant in the skin depth and it is equal to the differential permeability. In order to obtain differential permeability from μ_d - H curve (Fig. 12), surface magnetic field strength of the rail, H_o must be calculated:

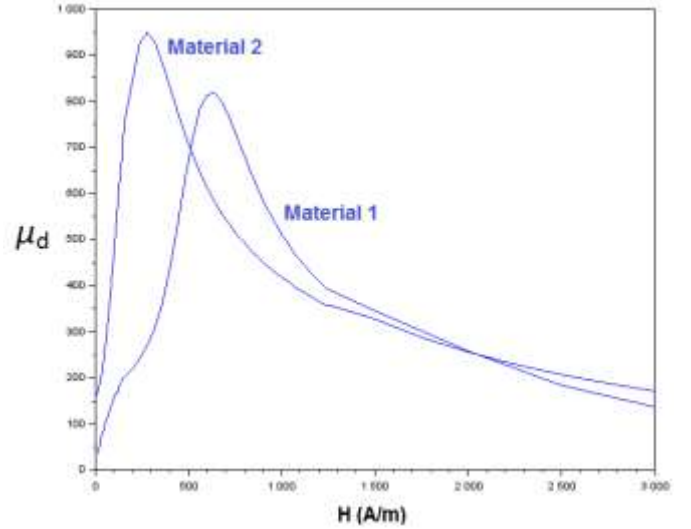


Fig. 12. Materials 1 and 2 - μ_d - H

VI. CONCLUSIONS

Different solid iron materials effects on the impedance of rails were presented. Analytical methods and FEM were used for the simulations.

Presented analytical methods are quite precise in comparison with FEM, which could be used for fast analysis of rails impedances. Approximate analytical methods were presented for two approximated models, circular and rectangular solid conductors.

Inductances and resistances were calculated at DC and AC currents with and without iron non-linearity effects. The material effects such as different electrical conductivities and B - H curves are not negligible at low and high frequencies.

The hysteresis effects have considerable effects on the resistances and the inductances of the rails.

REFERENCES

- [1] A. Alberto Dolara and Sonia Leva, "Calculation of Rail Internal Impedance by Using Finite Elements Methods and Complex Magnetic Permeability", *International Journal of Vehicular Technology* Volume 2009, Article ID 505246, 10 pages
- [2] Václav KOLÁŘ , Pavel BOJKO , Roman HRBÁČ, "Measurement of current flowing through a rail with the use of Ohm's method; determination of the impedance of a rail", *PRZEGLĄD ELEKTROTECHNICZNY*, ISSN 0033-2097, R. 89 NR 6/2013
- [3] J.C. Brown ; J. Allan ; B. Mellitt, "Calculation and measurement of rail impedances applicable to remote circuit fault currents", *IEE Proceedings B - Electric Power Applications* , Volume: 139, Issue: 4, Jul 1992
- [4] A. Mariscotti, P. Pozzobon, "Measurement of the internal impedance of traction rails at 50 Hz", *Instrumentation and Measurement IEEE Transactions on*, vol. 49, pp. 294-299, 2000, ISSN 0018-9456
- [5] A. Mariscotti, P. Pozzobon, "Measurement of the internal impedance of traction rails at audiofrequency", *Instrumentation and Measurement IEEE Transactions on*, vol. 53, pp. 792-797, 2004, ISSN 0018-9456.
- [6] A. Mariscotti, P. Pozzobon, "Resistance and internal inductance of traction rails at power frequency: a survey", *Vehicular Technology IEEE Transactions on*, vol. 53, pp. 1069-1075, 2004, ISSN 0018-9545.
- [7] F. Filippone, A. Mariscotti, P. Pozzobon, "The Internal Impedance of Traction Rails for DC Railways in the 100 kHz Frequency Range", *Instrumentation and Measurement IEEE Transactions on*, vol. 55, pp. 1616-1619, 2006, ISSN 0018-9456.
- [8] R. J. Hill, D. C. Carpenter, "Determination of rail internal impedance for electric railway traction system simulation", *IEE Proc. B*, vol. 138, no. 6, pp. 311-321, November 1991.
- [9] D. C. Carpenter; R. J. Hill, "The effects of magnetic saturation, hysteresis and eddy currents on rail track impedance Proceedings., Technical Papers Presented at the IEEE/ASME Joint Railroad Conference, Year: 1989, Pages: 73 - 79
- [10] R. J. Hill; D. C. Carpenter, Modelling of nonlinear rail impedance in AC traction power systems, *IEEE Transactions on Power Delivery*, Year: 1991, Volume: 6, Issue: 4. Pages: 1755 - 1761
- [11] H. M. Trueblood, G. Wascheck, "Investigation of rail impedances", *Electr. Eng.*, pp. 898-907, 1933.
- [12] Stoll, R. L., " Analysis of Eddy Currents", Published by Oxford University Press, 1974
- [13] <http://www.femm.info/wiki/Documentation/>
- [14] D. O'Kelly, "Hysteresis and eddy current losses in steel plates with nonlinear magnetization characteristics," *Proceedings of the IEE*, 119(11):1675-1676, November 1972